Molecular Structure of the Aluminum Halides, Al_2Cl_6, $AlCl_3$, Al_2Br_6, $AlBr_3$, and AlI_3, Obtained by Gas-Phase Electron-Diffraction and ab Initio Molecular Orbital Calculations

Kirsten Aarset,*,† Quang Shen,‡ Hanne Thomassen,§ Alan D. Richardson, and Kenneth Hedberg*

Contribution from the Department of Chemistry, Oregon State University, Corvallis, Oregon 97331

Received: October 27, 1998; In Final Form: January 8, 1999

Gas-phase electron-diffraction (GED) data together with results from ab initio molecular orbital and normal coordinate calculations have been used to determine the structures of the aluminum trihalides AlX_3 (X = Cl, Br, I) and the chloride and bromide dimers Al_2Cl_6 and Al_2Br_6. No monomeric species were detected in the vapors of Al_2Cl_6 at the experimental temperature of 150 °C, nor in Al_2Br_6 at167 °C, but the vapors of $AlCl_3$ at 400 °C and $AlBr_3$ at 330 °C contained respectively 29 (3)% and 7 (4)% dimer and the AlI_3 at 300 °C about 8% I_2. The known equilibrium symmetry of the dimers is D_{2h}, but the molecules have a very low-frequency, large-amplitude, ring-puckering mode that lowers the thermal average symmetry to C_{2v}. The effect of this large-amplitude mode on the interatomic distances was handled by dynamic models of the structures which consisted of a set of pseudoconformers spaced at even intervals along the ring-puckering angle 2Φ. The ring-puckering potential was assumed to be $V(\Phi) = V_4^0\Phi^4 + V_2^0\Phi^2$, and the individual pseudoconformers were given Boltzmann weights. The structures were defined in terms of the geometrically consistent r_α space constraining the differences between corresponding bond distances and bond angles in the different pseudoconformers to values obtained from ab initio calculations at the HF/6-311G(d) level. Results for the principal distances (r_g/Å), angles ($\angle_\alpha$,θ/deg), and potential constants (V_i^0/kcal mol deg^{-1}) from the combined GED/ab initio study for Al_2Cl_6/Al_2Br_6 with estimated 2σ uncertainties are Al−X_b = 2.250(3)/2.433(7), Al−X_t = 2.061(2)/2.234(4), X_bAlX_b = 90.0(8)/91.6(6), X_tAlX_t = 122.1(31)/122.1(31), $\langle\theta\rangle = 180 - 2\Phi$ = 165.5-(59)/158.2(91), V_4^0 = 0.0/75.0 (assumed), V_2^0 = 25.0/0.0 (assumed). The potential constants could not be refined; although the single-term values listed provide good fits, in each case combinations of quadratic and quartic terms also worked well. For the monomers $AlCl_3$, $AlBr_3$, and AlI_3 (D_{3h} symmetry assumed in r_α space) the distances (r_g/Å) with estimated 2σ uncertainties are Al−Cl = 2.062(3), Al−Br = 2.221(3), and Al−I = 2.459(5) Å. Vibrational force fields were evaluated for all molecules. The experimental, theoretical, and vibrational results are discussed.

Introduction

The molecular structures and vibrational behavior of the aluminum halide monomers and dimers, AlX_3 and Al_2X_6, have been extensively studied by various experimental methods (Raman[1−6] and IR[1,4−20] spectroscopy, gas-phase electron diffraction (GED[21−26]) and by ab initio molecular orbital calculations.[27−31] These studies confirm that the dimers in the gas phase have structures consistent with D_{2h} symmetry that may be pictured as two AlX_4 tetrahedra sharing a common edge (Figure 1). Also, there is little doubt that the monomers are planar with D_{3h} symmetry, although a pyramidal structure for the molecules (later shown to be unlikely[20,32,33]) has been proposed on the basis of an interpretation of infrared data.[11]

The initial intention of the present work was to evaluate the thermodynamics of the dissociation reactions of these halides by GED studies of the equilibria between monomers and dimers. An early study[24] of the stoichiometrically analogous $2NO_2 \rightleftarrows N_2O_4$ equilibrium suggested that useful information might be obtained by this method despite the obvious difficulties associated with gas expansion from a flow nozzle into a region of high vacuum. Several GED investigations of the aluminum and gallium halides were carried out by one of us (Q.S.) in parallel with the N_2O_4 work.[24] The difficulties mentioned have been more clearly revealed in a recent reanalysis of the early $NO_2-N_2O_4$ data,[34] as well as in results from aluminum halide data comprising both the early sets and sets newly made for this investigation. More specifically, aluminum halide experiments

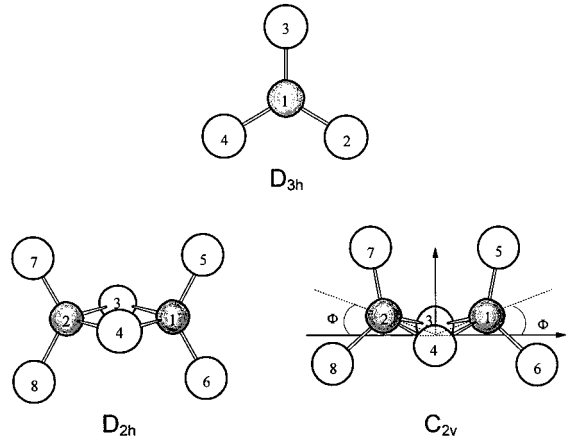

Figure 1. Molecular diagrams with atom numbering.

* Authors to whom correspondence should be addressed.
† Department of Chemistry, Norwegian University of Science and Technology, N-7034 Trondheim, Norway.
‡ Department of Chemistry, Colgate University, Hamilton, NY 13346.
§ Oslo College, Department of Engineering, N-0254 Oslo, Norway.

10.1021/jp9842042 CCC: $18.00
Published on Web 03/04/1999

TABLE 1: Conditions of Diffraction Experiments on Aluminum Halides

	$Al_2Cl_6/AlCl_3$		$Al_2Br_6/AlBr_3$		AlI_3
temperature/°C	150	400	167	330	300
no. long camera plates (LC)[a]	2	3	2	2	3
no. middle camera plates (MC)[a]	2	3	3	3	3
s_{min}/Å^{-1}, LC	2.25	2.25	2.25	2.25	2.25
s_{max}/Å^{-1}, LC	16.00	16.00	16.00	16.00	14.00
s_{min}/Å^{-1}, MC	8.25	8.25	8.25	8.25	8.25
s_{max}/Å^{-1}, MC	38.00	38.00	38.00	38.00	38.00
acceleration voltage/kV	60	60	61	60	60
calibration substance	CO_2	CO_2	CS_2	CO_2	CO_2
r_a(C═S)/Å or r_a(C═O)/Å	1.1626	1.1626	1.557	1.1626	1.1626
r_a(S··S)/Å or r_a(O··O)/Å	2.3244	2.3244	3.109	2.3244	2.3244
nominal electron wavelength/Å	0.049	0.049	0.048	0.049	0.049

[a] All plates were traced at least twice.

at different temperatures (different nozzle temperatures but the same bulk-sample temperature) showed that the equilibria are very sensitive to the experimental conditions and we were unable to get consistent results for the system compositions. However, we were able to obtain excellent structural parameter values for the two components of several of the systems, and since these both extend and differ in certain respects from the results of earlier work, a full presentation of our studies seems worthwhile.

Experimental Section

Although the early data for all molecules of this study were available, we decided to base our determinations only on newly gathered data: these new data included some sets obtained at nozzle-tip temperatures quite different from those used in the older experiments, and it was felt that this circumstance, in addition to other differing experimental conditions (e.g., accelerating voltages, electron-scattering factors, changed densitometer methods) would needlessly complicate comparisons.

Commercial samples of aluminum chloride (Aldrich, 99.99%), bromide (Aldrich, 99.99+%), and iodide (Cerac, 99.9%) were used in the current studies. The diffraction experiments were done with the Oregon State apparatus using an r^3 sector and Kodak electron-image plates developed for 12 min in D19 developer diluted 1:1. Nozzle-tip temperatures were 150 and 400 °C for the chloride, 167 and 330 °C for the bromide, and 300 °C for the iodide. Information about the experimental conditions for all data sets used in the present investigation are given in Table 1. The procedures for obtaining and analyzing the molecular intensity curves have been described elsewhere.[35−37] The complex scattering factors tabulated by Ross, Fink, and Hilderbrandt[38] were used in these and related calculations. The molecular intensity curves for aluminum chloride, bromide, and iodide, respectively, are given in Figures 2−4 and radial distribution (RD) curves in Figures 5 and 6.

Structure Analysis

Molecular Orbital Calculations. The mixture of monomer and dimer molecules, which have similar bond lengths and bond angles, in the vapors of these systems makes it difficult to extract reliable parameter values for each component separately. As is now common in cases difficult to analyze by GED alone, we elected to carry out ab initio molecular orbital calculations in order to provide a basis for reasonable parameter constraints. The dimer molecules were known[34] to undergo a large-amplitude bending motion around the hinge line joining the two bridge

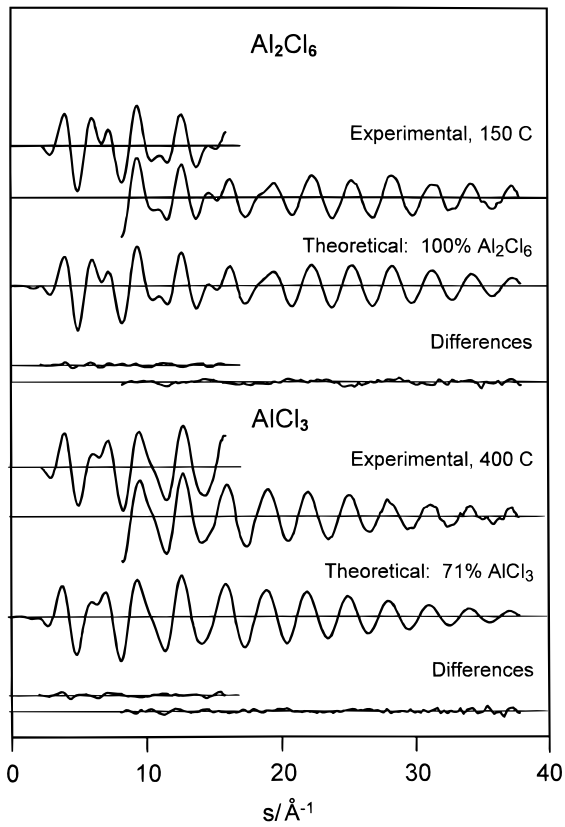

Figure 2. Intensity curves for Al_2Cl_6 and $AlCl_3$. The curves from 150 °C correspond to essentially pure Al_2Cl_6 and those from 400 °C to about 71% $AlCl_3$. Difference curves are experimental minus theoretical for the final models.

atoms as illustrated in Figure 1. In anticipation of models for the GED structure refinements, the dimer optimizations were carried out at selected values of the hinge, or ring-puckering, angle (Φ = 0, 5, 10, 15, 20°) based on an assumption of D_{2h} symmetry for the equilibrium structures (Φ = 0°) and C_{2v} for the others. The calculations were done with the program GAUSSIAN94[39] using several different basis sets and levels of theory to check the dependence of the planned constraints on these aspects of theory. The basis sets and levels of theory for Al_2Cl_6 were HF/6-31G(d), HF/6-31G(d,p), HF/6-31+G(d), HF/6-311G(d), HF/6-31G(d,p), HF/6-311+G(d), MP2/6-31G-(d), and MP2/6-311G(d)); and for Al_2Br_6 HF/6-311G(d) only. The distance and angle changes resulting from the HF/6-311G-(d) and MP2/6-311G(d) calculations are shown for Al_2Cl_6 in Figure 7 (the changes for Al_2Br_6 are similar) and the numerical data for all molecules are given in Table S1 of the Supporting Information. The monomer optimizations were based on an assumption of D_{3h} symmetry for the molecules. The calculations were done at the levels HF/6-31G(d), HF/6-311G(d), and HF/6-311+G(d) for $AlCl_3$; HF/6-311G(d) for $AlBr_3$; and LANL2DZ and HW(ECP)(d) for AlI_3 with the bases HW(ECP)(d)[40] for I and 6-31G(d) for Al. The results from these calculations are seen in Table S2 of the Supporting Information. Cartesian force fields and normal-mode wavenumbers of all monomers and dimers except AlI_3 were also calculated at the HF/6-311G(d) level. For AlI_3 the force field and wavenumbers were obtained for the LANL2DZ calculation cited.

Normal Coordinate Calculations. The program ASYM40[41] in an updated version that allows symmetrization of Cartesian force constants from ab initio programs was used to calculate symmetry force fields. The symmetry force fields were then adjusted to provide a fit to the observed wavenumbers recom-

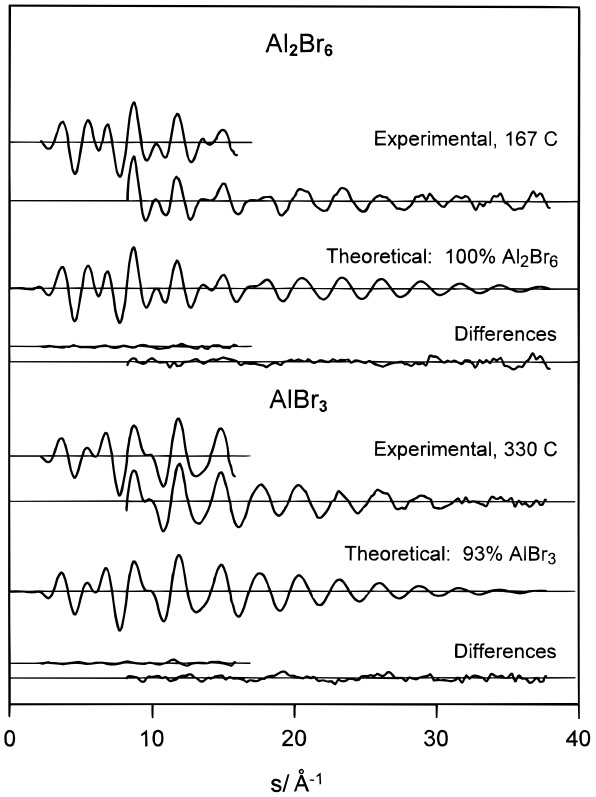

Figure 3. Intensity curves for Al_2Br_6 and $AlBr_3$. The curves from 167 °C correspond to essentially pure Al_2Br_6 and those from 330 °C to about 93% $AlBr_3$. Difference curves are experimental minus theoretical for the final models.

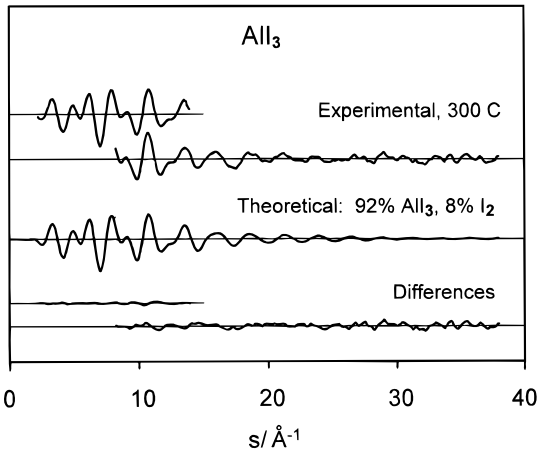

Figure 4. Intensity curves for AlI_3. The difference curves are experimental minus theoretical for the final model.

mended by Sjøgren et al.[7] except for the unobserved modes ν_5 (X_bAlX_b bend) and ν_{10} (ring puckering) in the dimers; for these modes we used the calculated wavenumbers. The wavenumbers for all molecules are given in Table 2, the force fields in Table 3, and the coordinates in Table 4. The usual corrections for interconversion of different distance types—perpendicular amplitudes K, centrifugal distortions δr, and root-mean-square amplitudes l—were calculated with ASYM40 from the symmetrized force fields.

The Models. The general model for the systems included allowance for the presence of both dimer and monomer. The equilibrium symmetry of the dimers was assumed to be D_{2h} and of the monomers D_{3h}, but an operational symmetry of C_{2v} for Al_2Br_6 was assumed for one model in order to investigate the effect of the large-amplitude ring-puckering motion referred

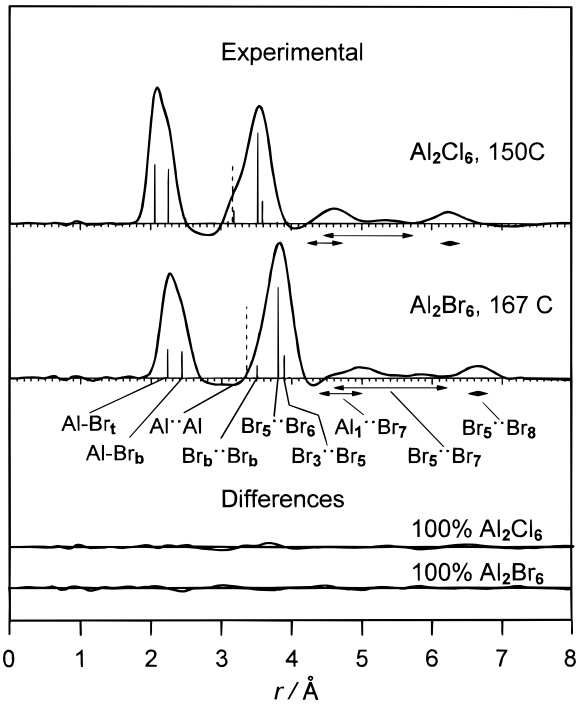

Figure 5. Radial distribution curves for the Al_2Cl_6 and Al_2Br_6 systems. Difference curves are experimental minus theoretical for the final models. The vertical bars indicate values of distances not much affected by the large-amplitude ring bending; their lengths are proportional to the weights of the terms. Dashed bars for the Al_2Br_6 system indicate dimer. The horizontal arrows show the ranges of distances strongly affected by the ring bending. The omitted distance labels for Al_2Cl_6 are similar to those for Al_2Br_6.

to earlier. (This bending mode is predicted theoretically to be of very low frequency—about 23 and 12 cm^{-1} for Al_2Cl_6 and Al_2Br_6, respectively.)

For the dimers a "rigid" model, i.e., one of D_{2h} symmetry not undergoing the large amplitude motion, was tested in some preliminary refinements, but as expected from our earlier studies[24] and theoretical calculations it did not fit the data very well. The preliminary refinements gave fairly good agreement for distances that are independent of, or little affected by, this ring-puckering mode, but very poor agreement for the other distances such as those between the terminal $-AlX_2$ groups. The rigid D_{2h} model was not considered further. However, if the D_{2h} symmetry restriction were to be relaxed to C_{2v} to allow bending around the bridging halogen atoms, considerable improvement could be expected. Such a model, which is "static" in respect to the ring puckering and which incorporated C_{2v} local symmetry for the $AlBr_4$ groups, was used in an earlier investigation[26] of Al_2Br_6 to obtain a good fit to experiment; we also tested it with our data for the bromide. The static model hardly provides a good description of the distance distributions dependent on the puckering in these floppy dimeric aluminum halide molecules, but refinement results based on it do give useful information about the magnitude of the puckering angle itself. (We ignored the static model in the analysis of Al_2Cl_6.) A more realistic model of these structures is one which takes into account the large-amplitude dynamics of the ring puckering. This type of model is based on the concept that large-amplitude motion may be represented by a set of appropriately weighted "pseudoconformers" distributed along the floppy coordinate such that the sum of the individual contributions approximates the results of the motion.[42] In the cases at hand these pseudocon-

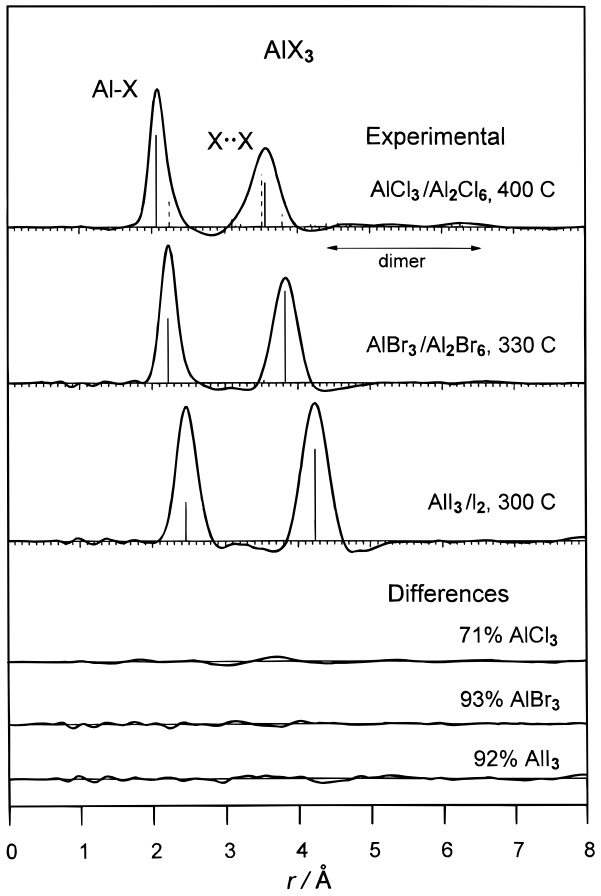

Figure 6. Radial distribution curves for $AlCl_3$, $AlBr_3$, and AlI_3 systems. Difference curves are experimental minus theoretical for the final models. Vertical solid bars indicate monomer distances, dashed bars indicate distances in Al_2Cl_6 not much affected by ring bending, and the horizontal arrow indicates the ranges of distances in Al_2Cl_6 sensitive to ring bending.

formers were weighted by Boltzmann factors, each determined by a two-term potential,

$$V(\Phi) = V_4^0\Phi^4 + V_2^0\Phi^2 \qquad (1)$$

where the angle Φ (Figure 1) is equal to $^1/_2(180 - \theta)$ with $\theta = \angle_{dih}(X_bAlX_b,X_bAlX_b)$ defined as 180° for coplanarity of the four atoms. Nine pseudoconformers defined by the angles $\Phi = 0$, $\pm 2\delta$, $\pm 3\delta$, $\pm 4\delta$, and $\pm 5\delta$, with $\delta = 5°$ for the chloride and $\delta = 6°$ for the bromide (only the monomeric form was detected for the iodide), were used to represent the ring-puckering motion. Each was treated as a distinct molecule undergoing the usual "frame" vibrations, i.e., all normal vibrations exclusive of the ring-puckering mode. The structure of each pseudoconformer was defined in terms of the parameters of the D_{2h} form ($\Phi = 0$) by adding the theoretical differences between the parameters of this form and those of the pseudoconformer in question as obtained by, or interpolated from, the ab initio optimizations found at the HF/6-311G(d) level (Table 5). The parameters for the D_{2h} form of the dimer were the average and the difference of the terminal (t) and bridge (b) bond lengths, $\langle r_d(Al-X)\rangle = [r_d(Al-X_t) + r_d(Al-X_b)]/2$, $\langle \Delta r_d(Al-X)\rangle = r_d(Al-X_b) - r_d(Al-X_t)$, and the bond angles $\angle_d(X_b-Al-X_b)$, and $\angle_d(X_t-Al-X_t)$. The monomer components of the systems required an additional structural parameter which was taken to be its bond length defined in terms of the D_{2h} form of the dimer via the difference between it and the terminal Al−X bond: $\Delta r_{m,d}(Al-X) = r_m(Al-X) - r_d(Al-X_t)$. Other parameters were a

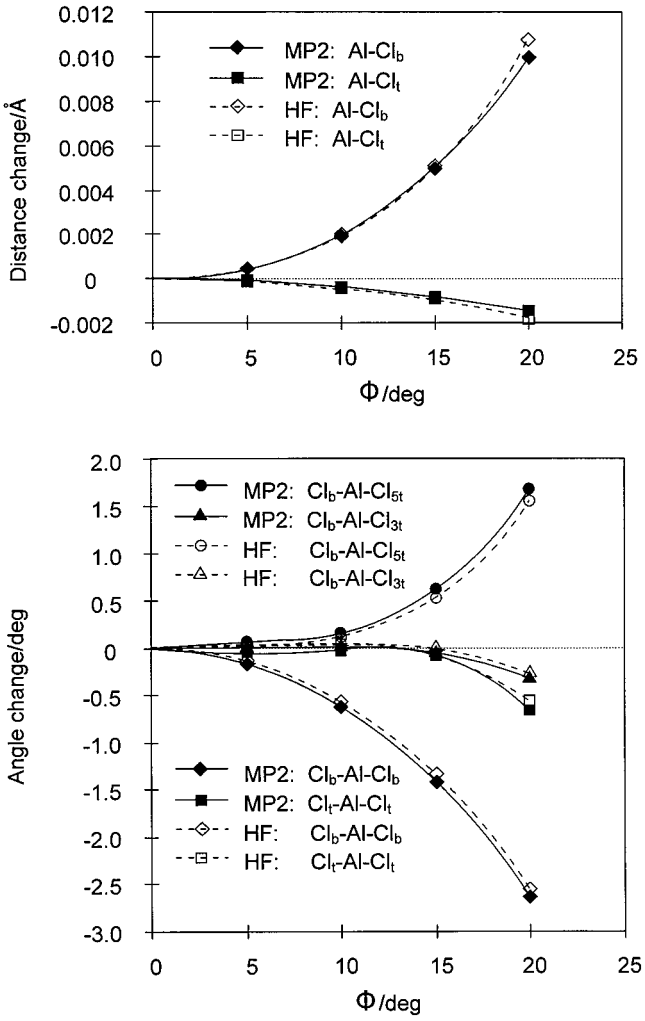

Figure 7. Parameter-value changes for pseudoconformers of Al_2Cl_6 obtained at the HF/6-311G(d) and MP2/6-311G(d) levels.

composition parameter for the systems of mixtures, the coefficients for the ring-puckering potential (V_2^0 and V_4^0), and a number of vibrational amplitudes.

Refinement Conditions. The structure refinements were carried out by least-squares[43] adjusting a theoretical $sI_m(s)$ curve simultaneously to the average intensity curves from each camera distance. The geometries of the molecules were defined by r_α and $\angle_\alpha$ parameters which were converted to the r_a type required in the scattered intensity formula with use of the calculated values of δr, K, and l mentioned in an earlier section. In each case the calculated differences between the values of the pseudoconformer parameters and those of the D_{2h} form (and the difference parameter defining the monomer) were applied to the r_α model with the assumption that Δr_α differs insignificantly from Δr_e. The vibrational amplitudes associated with distances characterizing each pseudoconformer were linked together throughout the set of pseudoconformers by differences constrained at values determined by the normal coordinate calculations. In the course of the work it was found necessary to group some of the vibrational amplitudes and to refine them as a single vibration parameter; in such cases the calculated theoretical differences between group members were imposed and maintained. The groupings are seen in Table 6.

Results for Al_2Cl_6 at 150 °C and Al_2Br_6 at 167 °C. Early experimental work[44] on the equilibrium vapor-phase composition of these compounds revealed that gaseous Al_2Cl_6 is 99.98% dimer at 180 °C and Al_2Br_6 is 99.3% dimer at 255 °C. Recent

TABLE 2: Observed and Calculated Wave Numbers/cm^{-1} for Aluminum Halides

		$Al_2Cl_6/AlCl_3$		$Al_2Br_6/AlBr_3$		AlI_3		
		obsd[a]	calcd[b]	obsd[a]	calcd[b]	obsd[a]	calcd[b]	assignment
				Dimers				
A_g	ν_1	511	512	409	410			Al−X_t str
	ν_2	337	340	203	205			Al−X_b str
	ν_3	219	223	139	143			ring bend
	ν_4	98	97	59	60			X_t−Al−X_t scis
A_u	ν_5[c]		66		41			X_b−Al−X_b bend
B_{1g}	ν_6	281	263	247	200			Al−X_b str
	ν_7	168	171	114	119			X_t−Al−X_t twist
B_{1u}	ν_8	626	615	507	495			Al−X_t str
	ν_9	178	182	110	114			X_t−Al−X_t rock
	ν_{10}[c]	25	23		12			ring puckering
B_{2g}	ν_{11}	614	604	489	486			Al−X_t asym str
	ν_{12}	115	119	85	82			X_t−Al−X_t rock
B_{2u}	ν_{13}	418	412	342	337			Al−X_b sym str
	ν_{14}	123	132	89	85			X_t−Al−X_t wag
B_{3g}	ν_{15}	105	122	76	75			X_t−Al−X_t twist
B_{3u}	ν_{16}	483	473	378	369			Al−X_t sym str
	ν_{17}	320	318	198	198			Al−X_b sym str
	ν_{18}	143	139	89	91			X_t−Al−X_t scis
				Monomers				
A_1'	ν_1	375	376	230	230	156	144	Al−X sym str
A_2''	ν_2	214	197	176	173	147	136	oop bend
E′	ν_3	616	613	503	496	427	392	Al−X asym str
E′	ν_4	148	145	94	94	66	63	X−Al−X bend

[a] Wavenumbers recommended by Sjøgren et al. (ref 7) except for $\nu_{10}(Al_2Cl_6)$ from ref 14. [b]From the HF/6-311G(d) level of theory (MP2/6-31G(d) for $AlCl_3$) multiplied by 0.9. [c]Blank entries are unobserved. Theoretical value used.

statistical thermodynamic data for the $Al_2Cl_6-AlCl_3$ system[14] support these experimental results. Thus, from the thermodynamic data we calculate an equilibrium constant K_p of about 7.6×10^{-8} and a composition of about 99.9% dimer for the decomposition reaction under the conditions of our experiments: 167 °C and an assumed total pressure of 8 Torr. Whether or not even approximate equilibrium exists under the conditions of our diffraction experiments is an open question. However, the initial structure refinements for these lower-temperature systems were consistent with the results just cited: they turned up no evidence for the presence of monomers.

The final refinements were completed with the assumption that monomers were absent. With this assumption all structure parameters for each dimer could be refined simultaneously except for a pair of amplitudes that had to be grouped. As expected, the coefficients of the ring-puckering potential turned out to be highly correlated so that a considerable range of combinations gave acceptable fits. Among these were ones that led to the quadratic term alone for Al_2Cl_6 ($V_4^0 = 0$; eq 1) and the quartic term alone for Al_2Br_6 ($V_2^0 = 0$). In the end these single-term potentials were adopted to describe the ring-puckering potentials. Small changes in the ring-puckering potentials, either through different values of the coefficients or by including the second terms, had little or no effect on the other structural parameters. The thermal-average parameter values from the final refinements are shown in Table 6 together with the ab initio HF/6-311G(d) optimized structures. Correlation matrixes are given in Table 7.

Results for $AlCl_3$ at 400 °C, $AlBr_3$ at 330 °C, and AlI_3 at 300 °C. Although analysis of the aluminum chloride system at 400 °C suggested the presence of about 30% dimer, it proved impossible to refine most of the structural parameters of this form. They were therefore constrained to the values obtained in the analysis of Al_2Cl_6 (data set at 150 °C), or in the case of $\Delta r_{m,d}$(Al−Cl) to the calculated value. Amplitudes for Al_2Cl_6 that were not tied to amplitudes in the monomer were constrained to the calculated values. Reasonable changes in the assumptions involving the Al_2Cl_6 structure did not change the structure of the monomer significantly. In the refinement of $AlBr_3$ where only about 7% of the dimer was found, none of

TABLE 3: Symmetry Force Constants for Aluminum Halides[a]

		Al_2Cl_6				Al_2Br_6			
		F_i	F_j	F_k	F_l	F_i	F_j	F_k	F_l
A_g	F_1	2.840				2.258			
	F_2	0.165	1.386			0.151	1.123		
	F_3	−0.043	0.131	0.642		−0.038	0.096	0.539	
	F_4	0.037	−0.120	0.006	0.552	0.040	−0.110	0.005	0.541
A_u	F_5	0.341				0.344			
B_{1g}	F_6	0.917				0.880			
	F_7	0.388	0.595			0.299	0.536		
B_{1u}	F_8	2.709				2.177			
	F_9	0.142	0.419			0.134	0.423		
	F_{10}	0.0	0.0	0.139		−0.003	−0.11	0.091	
B_{2g}	F_{11}	2.680				2.123			
	F_{12}	0.169	0.361			0.209	0.454		
B_{2u}	F_{13}	1.328				1.132			
	F_{14}	0.033	0.673			0.138	0.783		
B_{3g}	F_{15}	0.245				0.336			
B_{3u}	F_{16}	2.886				2.306			
	F_{17}	0.309	1.287			0.268	1.071		
	F_{18}	0.085	−0.172	0.543		0.070	−0.152	0.519	

		$AlCl_3$		$AlBr_3$		AlI_3	
		F_1	F_2	F_1	F_2	F_1	F_2
A_1'	F_1	2.897		2.459		1.820	
A_2''	F_2	0.368		0.327		0.305	
E′	F_3	2.673		2.186		1.698	
	F_4	−0.125	0.392	−0.124	0.384	−0.118	0.379

[a] Stretches in aJ/Å^2; bends in aJ/rad^2; stretch−bends in aJ/(Å·rad).

TABLE 4: Symmetry Coordinates for Aluminum Halides[a]

species	symmetry coordinates
	Al_2X_6
A_g	$S_1 = (1/2)\Delta(r_{15} + r_{16} + r_{27} + r_{28})$
	$S_2 = (1/2)\Delta(r_{13} + r_{14} + r_{23} + r_{24})$
	$S_3 = (1/2)\Delta(\alpha_{314} + \alpha_{324} - \alpha_{132} - \alpha_{142})$
	$S_4 = (1/\sqrt{2})\Delta(\alpha_{516} + \alpha_{728})$
A_u	$S_5 = (1/\sqrt{8})\Delta(-\alpha_{315} + \alpha_{316} + \alpha_{327} - \alpha_{328} + \alpha_{415} - \alpha_{416} - \alpha_{427} + \alpha_{428})$
B_{1g}	$S_6 = (1/2)\Delta(r_{13} - r_{14} - r_{23} + r_{24})$
	$S_7 = (1/\sqrt{8})\Delta(\alpha_{315} + \alpha_{316} - \alpha_{327} - \alpha_{328} - \alpha_{415} - \alpha_{416} + \alpha_{427} + \alpha_{428})$
B_{1u}	$S_8 = (1/2)\Delta(r_{15} - r_{16} + r_{27} - r_{28})$
	$S_9 = (1/\sqrt{8})\Delta(\alpha_{315} - \alpha_{316} + \alpha_{327} - \alpha_{328} + \alpha_{415} - \alpha_{416} + \alpha_{427} - \alpha_{428})$
	$S_{10} = \Delta\tau_{1324}$
B_{2g}	$S_{11} = (1/2)\Delta(r_{15} - r_{16} - r_{27} + r_{28})$
	$S_{12} = (1/\sqrt{8})\Delta(\alpha_{315} - \alpha_{316} - \alpha_{327} + \alpha_{328} + \alpha_{415} - \alpha_{416} - \alpha_{427} + \alpha_{428})$
B_{2u}	$S_{13} = (1/2)\Delta(r_{13} - r_{14} + r_{23} - r_{24})$
	$S_{14} = (1/\sqrt{8})\Delta(\alpha_{315} + \alpha_{316} + \alpha_{327} + \alpha_{328} - \alpha_{415} - \alpha_{416} - \alpha_{427} - \alpha_{428})$
B_{3g}	$S_{15} = (1/\sqrt{8})\Delta(\alpha_{315} - \alpha_{316} + \alpha_{327} - \alpha_{328} - \alpha_{415} + \alpha_{416} - \alpha_{427} + \alpha_{428})$
B_{3u}	$S_{16} = (1/2)\Delta(r_{15} + r_{16} - r_{27} - r_{28})$
	$S_{17} = (1/2)\Delta(r_{13} + r_{14} - r_{23} - r_{24})$
	$S_{18} = (1/\sqrt{2})\Delta(\alpha_{516} - \alpha_{728})$
	AlX_3
A_1'	$S_1 = (1/\sqrt{3})\Delta(r_{12} + r_{13} + r_{14})$
A_2''	$S_2 = \Delta\tau_{1234}$
E′	$S_{3a} = (1/\sqrt{6})\Delta(2r_{12} - r_{13} - r_{14})$
	$S_{3b} = (1/\sqrt{2})\Delta(r_{13} - r_{14})$
E′	$S_{4a} = (1/\sqrt{6})\Delta(-\alpha_{214} + 2\alpha_{413} - \alpha_{312})$
	$S_{4b} = (1/\sqrt{2})\Delta(\alpha_{214} - \alpha_{312})$

[a] Atom numbering from Figure 1.

TABLE 5: Results of Ab Initio HF/6-311G(d) Optimizations for Structures of Al_2Cl_6 and Al_2Br_6[a]

Φ[b]	$r(Al-Cl_b)$	$r(Al_1-Cl_5)$	$r(Al_1-Cl_6)$	$\angle(Cl_tAlCl_t)$	$\angle(Cl_bAlCl_5)$	$\angle(Cl_bAlCl_6)$	$\angle(Cl_bAlCl_b)$	$\angle(AlCl_bAl)$	
					Al_2Cl_6				$E_h + 3241.0$
0	2.278	2.077	2.077	121.76	110.25	110.25	89.32	90.68	−0.3624824
5	2.278	2.077	2.077	121.78	110.25	110.28	89.18	90.38	−0.3622023
10	2.280	2.076	2.077	121.80	110.36	110.32	88.76	89.48	−0.3612750
15	2.283	2.075	2.077	121.68	110.77	110.27	88.00	88.03	−0.3593881
20	2.289	2.073	2.077	121.20	111.81	109.98	86.78	86.14	−0.3558512
					Al_2Br_6				$E_h + 15918.0$
0	2.454	2.246	2.246	120.72	110.20	110.20	91.42	88.58	−0.5285364
5	2.454	2.246	2.246	120.75	110.29	110.17	91.21	88.36	−0.5283579
10	2.456	2.245	2.246	120.78	110.42	110.19	90.77	87.53	−0.5277403
15	2.459	2.244	2.246	120.67	110.93	110.06	89.95	86.21	−0.5263916
20	2.464	2.241	2.247	120.19	112.08	109.67	88.74	84.41	−0.5236734

[a] Distances in angstroms and angles in degrees. [b] Ring-puckering angle.

TABLE 6: Average Experimental (Dynamic Model) and Theoretical Parameter Values for Al_2Cl_6 and Al_2Br_6[a]

	Al_2Cl_6						Al_2Br_6					
	experimental (150 °C)				theoretical[b]		experimental (167 °C)				theoretical[b]	
parameters	$r_\alpha/\angle_\alpha$				$r_e,/\angle_e$		$r_\alpha,/\angle_\alpha$				$r_e,/\angle_e$	
$\langle r(Al-X)\rangle$	2.145(2)				2.177		2.323(4)				2.350	
$\Delta r(Al-X)$	0.195(3)				0.201		0.205(7)				0.208	
$\angle X_bAlX_b$	90.0(8)				89.3		91.6(6)				91.4	
$\angle X_tAlX_t$	122.1(31)				121.8		122.1(31)				120.7	
$V_4{}^{0\,c}$	0				105.7		[75.0]				98.3	
$V_2{}^{0\,c}$	[25.0]				21.2		0				13.0	
$\langle\theta\rangle^d$/deg	165.5(59)				180.0		158.2(91)					
	r_α	r_a	r_g	l_α	r_e	l_α	r_α	r_a	r_g	l_α	r_e	l_α
$r(Al-X_b)$	2.242(3)	2.247	2.250	0.078 } (4)	2.278	0.079	2.426(7)	2.431	2.433	0.084 } (5)	2.454	0.082
$r(Al-X_t)$	2.048(2)	2.059	2.061	0.052 }	2.077	0.052	2.221(4)	2.233	2.234	0.058 }	2.246	0.057
$r(Al\cdot\cdot Al)$	3.144(32)	3.147	3.152	0.119(72)		0.100	3.299(28)	3.303	3.307	[0.116]		0.115
$r(X_3\cdot\cdot X_4)$	3.173(31)	3.178	3.180	0.085(22)		0.088	3.501(27)	3.504	3.507	0.104(19)		0.100
$r(X_7\cdot\cdot X_8)$	3.584(54)	3.593	3.596	0.112 } (11)		0.119	3.887(60)	3.895	3.899	0.131 } (12)		0.132
$r(X_3\cdot\cdot X_5)$	3.516(20)	3.518	3.524	0.144 }		0.151	3.799(20)	3.801	3.807	0.155 }		0.154
$r(Al_1\cdot\cdot X_7)$	4.499(33)	4.499	4.506	0.176(62)		0.144	4.766(25)	4.770	4.775	[0.157]		0.155
$r(X_5\cdot\cdot X_7)$	5.111(86)	5.117	5.122	[0.169]		0.170	5.411(86)	5.420	5.424	0.155(67)		0.189
$r(X_6\cdot\cdot X_7)$	6.226(43)	6.227	6.231	[0.166]		0.167	6.622(38)	6.624	6.628	0.164(62)		0.173
R^e	0.111							0.202				

[a] Distances (r) and rms amplitudes (l) in angstroms, angles ($\angle$) in degrees. Values in parentheses are estimated 2σ and include estimates of systematic error; values in braces refined as a group. [b] D_{2h} equilibrium symmetry; HF/6-311G(d). [c] Coefficients of ring-bending potential; see text. Units: V_40 in kcal mol^{-1} rad^{-4}, V_20 in kcal mol^{-1} rad^{-2}. [d] Average ring-puckering angle, $180 - \langle 2\Phi\rangle$; see Figure 1. [e] Quality-of-fit factor: $R = [\Sigma_i w_i \Delta_i 2/\Sigma_i I_i(\text{obsd})^2]^{1/2}$ where $\Delta_i = I_i(\text{obsd}) - I_i(\text{calcd})$ with $I_i = s_i I_i$.

TABLE 7: Correlation Matrixes (×100) for Parameters of Al_2Cl_6 at 150 °C and Al_2Br_6 at 167 °C[a]

	σ_{LS}[b] ×100		r_1	Δr_2	$\angle_3$	$\angle_4$	l_5	l_6	l_7	l_8	l_9	l_{10}	l_{11}
1 $\langle r_d(Al-X)\rangle$	0.067	0.15	100	*56*	*4*	*30*	*5*		*14*	*−25*		*−1*	*14*
2 $\Delta\, r_d(Al-X)$	0.11	0.23	63	100	*−13*	*17*	*24*		*12*	*2*		*2*	*11*
3 $\angle(X_b-Al-X_b)$	40.	31.	−6	−12	100	*−66*	*−12*		*−11*	*34*		*>1*	*−11*
4 $\angle(X_t-Al-X_t)$	109.	111.	16	10	−44	100	*3*		*−7*	*−81*		*1*	*4*
5 $l(Al-X_b)$	0.057	0.15	13	32	−3	−3	100		*11*	*23*		*5*	*11*
6 $l(Al\cdot Al)$	2.5		>1	−1	−68	11	−3	100					
7 $l(X_b\cdot X_b)$	0.76	0.64	11	12	50	−20	9	−80	100	*29*		*−1*	*8*
8 $l(X_t\cdot X_t)$	0.35	0.39	−15	−2	23	−89	18	−1	13	100		*1*	*13*
9 $l(Al\cdot X_t)$	2.2		−1	1	6	−5	3	−6	5	7	100		
10 $l(X_t\cdot X_t)_{cis}$		2.2										100	*>1*
11 $l(X_t\cdot X_t)_{trans}$		2.4											100

[a] Values for Al_2Cl_6 in regular typeface, for Al_2Br_6 in italics. [b] Standard deviations from least squares. Units: distances and amplitudes in angstroms, angles in degrees, $V_4{}^0$ in kcal rad^{-4} mol^{-1}, and $V_2{}^0$ in kcal rad^{-2} mol^{-1}.

the dimer parameters could be refined. They were constrained at the values obtained for pure Al_2Br_6 at 167 °C, or in the cases of $\Delta r_d(Al-Br)$ and $\Delta r_{m,d}(Al-Br)$, at the calculated values. Dimer amplitudes not tied to amplitudes in the monomer were constrained at the calculated values. Because of the small amounts of dimer present, variations in these constraints had little effect on the structure of the monomer. In the analysis of the AlI_3 data there was no indication of the presence of dimer; instead, there was evidence of a small amount, about 7%, of I_2 presumably resulting from thermal decomposition of the monomer. The parameters of the I_2 molecule were constrained to the values $r_a = 2.674$ Å and $l = 0.045$ Å. The final experimental and theoretical results are shown in Table 8. Correlation matrixes are given in Table 9. Theoretical intensity curves for the final models together with experimental and difference curves are shown for the $Al_2Cl_6/AlCl_3$ and $Al_2Br_6/AlBr_3$ systems in Figures 2 and 3 and for the AlI_3 system in Figure 4. Corresponding radial distribution curves are seen in Figures 5 and 6.

TABLE 8: Structural Parameter Values for $AlCl_3$, $AlBr_3$, and AlI_3[a]

	experimental				theoretical[b]	
	r_α	r_a	r_g	l	r_e	l
this work (exptl at 400 °C)						
r(Al−Cl)	2.052(3)	2.061	2.063	0.063(3)	2.071	0.062
r(Cl··Cl)	3.554(4)	3.553	3.559	0.140(7)	3.588	0.145
χ[c]	0.71(3)					
ref 25 (877 °C)						
r(Al−Cl)			2.068(4)	0.074(3)		
r(Cl··Cl)			3.571(9)	0.187(6)		
χ			[100]			
ref 25 (1137 °C)						
r(Al−Cl)			2.074(4)	0.083(2)		
r(Cl··Cl)			3.567(10)	0.198(7)		
χ			[100]			
this work (330 °C)						
r(Al−Br)	2.210(3)	2.219	2.221	0.068(4)	2.235	0.064
r(Br··Br)	3.828(6)	3.827	3.833	0.151(8)	3.871	0.149
χ[c]	0.92(4)					
ref 26 (557 °C)						
r(Al−Br)			2.231(5)	0.075(2)		
r(Br··Br)			3.842(8)	0.169(4)		
χ			[100]			
this work (300 °C)						
r(Al−I)	2.449(5)	2.459	2.461	0.075(10)	2.534	0.070
r(I··I)	4.241(8)	4.240	4.247	0.169(10)	4.389	0.166
χ[c]	0.94(5)					

[a] Distances (r) and amplitudes (l) in angstroms. Quantities in parentheses are 2σ estimates. [b] HF/6-311G(d) for $AlCl_3$ and $AlBr_3$, and LANL2DZ for AlI_3; see text. [c] Mole fraction. Second components were dimers for $AlCl_3$ and $AlBr_3$, and I_2 for AlI_3. See text.

TABLE 9: Correlation Matrixes (×100) for Parameters of Monomers: $AlCl_3$ at 400 °C, $AlBr_3$ at 330 °C, and AlI_3 at 300 °C

	σ_{LS}[a,b] × 100	r_1	l_2	l_3	l_4	l_5	X_6
1 r_m(Al−Cl)	0.054	100					
2 l_m(Al−Cl)	0.051	5	100			$AlCl_3$	
3 l_m(Cl·Cl)	0.165	−13	24	100			
4 l_d(Cl_b·Cl_b)	1.01	1	−2	2	100		
5 l_d(Al·Cl_t)	5.27	−6	−2	6	−1	100	
6 X_m[c]	1.07	59	9	−19	−10	−6	100

	σ_{LS}[a,b] × 100	r_1	l_2	l_3	X_4	
1 r_m(Al−Br)	0.093	100				
2 l_m(Al−Br)	0.127	9	100			$AlBr_3$
3 l_m(Br·Br)	0.201	−8	36	100		
4 X_m[c]	1.56	50	18	−15	100	

	σ_{LS}[a,b] × 100	r_1	l_2	l_3	l_4	X_5
1 r_m(Al−I)	0.141	100				
2 l_m(Al−I)	0.348	10	100			AlI_3
3 l_m(I·I)	0.273	−3	50	100		
4 X_m[c]	1.63	27	50	8	−82	100

[a] Standard deviations from least squares. [b] Units: distances (r) and amplitudes (l) in angstroms. [c] Mole fraction monomer.

Discussion

Vibrational Properties. With the exception of ν_6 in the dimers, the calculated (from the HF/6-311G(d) level of theory) and observed vibrational wavenumbers for the aluminum halides are in good agreement (Table 2); similar differences for ν_6 have been reported from earlier theoretical calculations.[28] The ring-puckering wavenumbers (ν_{10}) are notable for their small values, as are the corresponding symmetrized force constants (Table 3). The force constants for all the molecules are similar to those reported before.[7] An interesting feature is the parallel similarity of the stretching constants for the chloride and bromide monomers to their terminal-bond counterparts in the dimers, and the similarity of the corresponding bond lengths. However, although the force fields themselves are reasonable and consistent among the molecules of similar type, our main interest in them concerned their use for the calculation of the several corrections (distance, perpendicular amplitudes, etc.) and root mean square amplitudes of vibration used in the diffraction analysis. Reasonable differences in force fields had no significant effect on the values of these quantities. As is seen from Tables 6 and 8, the calculated and observed values are in good agreement.

Molecular Structures. One of the most interesting aspects of the aluminum halide dimers is the puckering motion of the four-membered ring. This motion is characterized mainly by a bending around an axis through the bridging halogen atoms and is of large amplitude, giving rise to average ring-puckering angles, i.e., deviations from ring planarity, of about 15° for Al_2Cl_6 and 22° for Al_2Br_6. The puckering motion leads to average values for the distances most affected by it—the trans X··X, the cis X··X, and the Al·X—that are significantly smaller than those corresponding to the D_{2h} equilibrium conformation. For example, in Al_2Br_6 the average r_g values for $(Br\cdot\cdot Br)_{trans}$, $(Br\cdot\cdot Br)_{cis}$, and Al·Br are respectively 6.63, 5.42, and 4.77 Å, whereas the corresponding D_{2h} values are 6.73, 5.49, and 4.82 Å. More important for the interpretation of the diffraction data is the fact that these three distances change dramatically during the course of the puckering motion which washes out their contribution to the scattered intensities. In the Al_2Br_6 example the ranges of the $(Br\cdot\cdot Br)_{trans}$, $(Br\cdot\cdot Br)_{cis}$, and Al·Br distances that encompass about 85% of the pseudoconformers are 0.13, 1.70, and 0.60 Å. These ranges are illustrated in Figure 5 by the horizontal arrows. Slightly smaller ranges are found for Al_2Cl_6.

The ab initio calculations carried out for Al_2Cl_6 with different basis sets and levels of theory predict similar *differences* between the values of a parameter for given pairs of pseudoconformers. As expected, however, the predicted values of the parameters themselves vary appreciably, especially with change in the level of theory. The examples shown in Figure 7 are typical of these effects; more details are found in Table S1 of the Supporting Information. The ring-puckering potentials were also found to be theoretically similar for different basis sets, but the minima are slightly broader from the MP2 level of theory than from the HF level. These trends are expected to be similar for Al_2Br_6. The experimental values for the bond lengths of the molecules comprising the aluminum chloride and aluminum bromide systems are generally 0.02−0.04 Å smaller than the theoretical values, a relationship that is qualitatively consistent with observation for many organic molecules. The agreement between theory and experiment is best for the higher levels of theory e.g., MP2/6-311G(d). The theory−experiment agreement for the bond angles is better.

The results summarized in Table 6 are those obtained from a model designed to take account of the dynamics of the ring-puckering motion. Results from the static model for Al_2Br_6 are listed in Table 10 together with ones from the earlier study[26] based on this model and those from our dynamic model. The bond lengths obtained for Al_2Br_6 in our work from the two model types are virtually identical, but the bond angles and the average bending angles of the four-membered ring differ slightly. The distances dependent on the ring-puckering angle and the amplitudes associated with them are not directly

TABLE 10: Summary of Results from Different Models of Al_2Br_6[a]

	this work (167 °C)					
	dynamic model		static model		Hargittai et al.[b] static model (87 °C)	
parameters	r_g; $\angle_\alpha$	l	r_g; $\angle_\alpha$	l	r_g; $\angle_\alpha$	l
$r(Al-Br_b)$	2.433(7)	0.084 } (6)	2.434(7)	0.084(6)	2.421(5)	0.079(2)
$r(Al-Br_t)$	2.234(4)	0.058 }	2.234(4)	0.058(5)	2.227(5)	0.053(2)
$\angle Br_bAlBr_b$	91.6(6)		92.5(8)		93.3(2)	
$\angle Br_tAlBr_t$	122.1(31)		120.5(44)		119.6(7)	
$\langle\theta\rangle$[c]	158.2(91)		157.8(34)		141.4(13)	
$r(Al\cdot\cdot Al)$	3.305(31)	[0.115]	3.298(31)	[0.115]	3.271(5)	[0.115]
$r(Br_3\cdot\cdot Br_4)$	3.510(29)	0.102(19)	3.511(26)	0.106(19)	3.518(4)	0.108(5)
$r(Br_7\cdot\cdot Br_8)$	3.896(65)	0.132 } (12)	3.869(86)	0.138 } (11)	3.848(10)	0.117 } (1)
$r(Br_3\cdot\cdot Br_5)$	3.809(21)	0.154 }	3.819(30)	0.160 }	3.810(4)	0.154 }
$r(Al_1\cdot\cdot Br_8)$[d]	4.776(26)	[0.155]	5.046(41)	0.165(74)	4.999(10)	0.203(11)[f]
$r(Al_1\cdot\cdot Br_7)$[d]			4.519(66)	0.202 } (104)	4.558(15)	0.325(35)
$r(Br_5\cdot\cdot Br_7)$[e]	5.429(90)	0.155(65)	4.696(177)	0.236 }	4.835(36)	0.297(11)[f]
$r(Br_6\cdot\cdot Br_8)$[e]			6.227(157)	[0.173]	6.123(33)	0.523(98)
$r(Br_6\cdot\cdot Br_7)$	6.631(39)	0.163(68)	6.639(62)	0.177(54)	6.664(9)	0.186(7)
R[g]	0.202		0.207			

[a] Distances (r) and amplitudes (l) in angstroms, angles ($\angle$ and θ) in degrees. Values in parentheses are 2σ and include estimates of systematic uncertainty; those in square brackets were assumed, and those in curly brackets were refined as groups. [b] Ref 26. [c] $\langle\theta\rangle = 180 - \langle 2\Phi\rangle$; see Figure 1. [d,e] Equivalent distances in dynamic (large-amplitude) model. [f] Refined as a group. [g] See Table 6.

comparable in the two models, but the distance averages indicated by the curly brackets in the dynamic model are roughly equal to the averages of the two components in the static model. The parameter values from the two static models may be compared directly, and are seen to be in good agreement when account is taken of the uncertainties attached to each. The largest apparent difference between the two sets of results for this model is the relative size of the uncertainties: except for those associated with the first four parameters, which were used to define the structure, ours are generally much larger. Somewhat larger uncertainties might also be expected in our work because of the higher temperature of our experiment and thus a greater washing out of the distances sensitive to the ring puckering.

As was mentioned in an earlier section, structural results for several of the aluminum halide systems had been obtained in this laboratory in an unpublished investigation carried out over two decades ago.[34] The following are r_a/Å and $\angle_\alpha$/deg values for the new/old investigations. Al_2Cl_6: Al−Cl_t, 2.059(2)/2.065(2); Al−Cl_b, 2.247(3)/2.252(4); Cl_tAlCl_t, 122.1(31)/123.4(16); Cl_bAlCl_b, 90.0(8)/91.0(5); $\langle\theta\rangle$, 165.5(59)/156.6(60). Al_2Br_6: Al−Br_t, 2.233(4)/2.222(5); Al−Br_b, 2.431(7)/2.414(8); Br_tAlBr_t, 1221.1(31)/122.8(33); Br_bAlBr_b, 91.6(6)/92.3(9); $\langle\theta\rangle$, 158.2(91)/156.7(60). AlI_3, Al−I, 2.449(5)/2.459(13). It is pleasing that the two sets of results agree well, for the present work drew on a much improved experiment, and on advanced auxiliary aids such as constraints from ab initio and normal coordinate calculations, that were not available before.

Table 8 includes results for $AlCl_3$ and $AlBr_3$ from two previous GED investigations. The sample temperatures in these studies were in each case considerably higher than in ours, and it is particularly satisfying to note that both the bond lengths and the vibrational amplitudes for both distances in each molecule are seen to increase with increased sample temperature. The effects of vibrational averaging can also be seen in the distance values. For example, in our work the apparent bond angles calculated from the r_g distances are respectively 119.3° instead of 120° for all three molecules. Equivalent or larger differences are found from the data of the other investigations, especially those carried out at higher temperatures.

According to ab initio HF/6-311G(d) theory the equilibrium lengths (r_e) of the Al−Cl and Al−Br bonds in the monomers should be shorter than the terminal Al−X bonds in the dimers by 0.006 and 0.011 Å, respectively. The corresponding experimental r_g differences are −0.001 and 0.013 Å. This is good agreement; however, the experimental bond lengths are affected by thermal averaging of molecular vibration and a better comparison requires distances of the same type. A rough estimate of "experimental" r_e values is obtained[45] from the formula $r_e = r_g - (3/2)al^2$ where $a \simeq 2.0$ Å^{-1} is the Morse anharmonicity constant for bonds and l^2 is the mean-square amplitude of vibration. These differences ($r_{d,t} - r_m$) are −0.018 Å for the chlorides and −0.010 Å for the bromides and thus differ from theoretical prediction by slightly more than 0.02 Å. The experimental and theoretical r_e differences between the bridge and terminal bonds in the dimers, $r_b - r_t$, are also in good agreement; they are respectively 0.177 and 0.201 Å for Al_2Cl_6, and 0.185 and 0.208 Å for Al_2Br_6.

Finally, it is worth noting that a simple picture of the bonding in these molecules may be had from the classic Pauling bond numbers[46] calculated with the Schomaker−Stevenson electronegativity correction.[47] The bond numbers are 1.2 and 0.6 for Al−Cl_t and Al−Cl_b in Al_2Cl_6, 1.2 for Al−Cl in $AlCl_3$, 1.1 and 0.5 for Al−Br_t and Al−Br_b in Al_2Br_6, 1.1 for Al−Br in $AlBr_3$, and 1.0 for Al−I in AlI_3, from which the Al−Cl_t and Al−Br_t bonds in the dimers and the bonds in the corresponding monomers have respectively about 20% and 10% double-bond character and the Al−I bonds are essentially single bonds. The aluminum atom thus forms the equivalent of 3.7 single bonds in $AlCl_3$, 3.3 single bonds in $AlBr_3$, and 3.0 single bonds in AlI_3; the differences are consistent with the abilities of the halogen atoms to engage in π back-bonding as well as with the decreasing values of the stretching symmetry force constants in this series of molecules. Although a bit more complicated, the picture for Al_2Cl_6 and Al_2Br_6 is similar. Each aluminum atom has a bond-number total of 3.7 in Al_2Cl_6 and 3.2 in Al_2Br_6, but in each case only one-third of these totals derives from the two bridge bonds. The bonding of the aluminum atoms to the two bridge atoms may thus be seen as the equivalent of the bonding to one of the terminal bonds.

Acknowledgment. This work was supported by the National Science Foundation under grants CHE95-23581 and GP27763X. The Norwegian Research Council (NFR) for a fellowship to K.A. Financial support from the Norwegian National Super-

computer Committee (TRU) for a grant of computing time on the Cray J90 is also gratefully acknowledged.

Supporting Information Available: Tables of ab initio results for the structures of $AlCl_3$, $AlBr_3$, and AlI_3 and for the structures of pseudoconformers of Al_2Cl_6 and Al_2Br_6; and of the averaged molecular intensities from each of the camera distances for all molecules. This material is available free of charge via the internet at http://pubs.acs.org.

References and Notes

(1) Tomita, T.; Sjøgren, C. E.; Klæbø, P.; Papatheodorou, G. N.; Rytter, E. *J. Raman Spectrosc.* **1983**, *14*, 415.
(2) Gerding, H.; Smith, E. *Z. Phys. Chem.* **1941**, *B50*, 171.
(3) Beattie, I. R.; Horder, J. R. *J. Chem. Soc. A* **1969**, 2655.
(4) Tranquille, M.; Fouassier, M. *J. Chem. Soc., Faraday Trans II* **1980**, *76*, 26.
(5) Beattie, I. R.; Gilson, T.; Ozin, G. A. *J. Chem. Soc. A* **1968**, 813.
(6) Klæbø, P.; Rytter, E.; Sjøgren, C. E.; Tomita, T. *Soc. Photo-Opt. Instrum. Eng.* **1981**, *289*, 283.
(7) Sjøgren, C. E.; Klæbø, P.; Rytter, E. *Spectrochim. Acta A* **1984**, *40*, 457.
(8) Klæbø, P.; Rytter, E.; Sjøgren, C. E. *J. Mol. Struct.* **1984**, *113*, 213.
(9) Pong, R. G. S.; Shirk, A. E.; Shirk, J. S. *Ber. Bunsen-Ges. Phys. Chem.* **1978**, *82*, 79.
(10) Einarsrud, M.-A.; Rytter, E. *Proc. Electrochem. Soc.* **1987**, *87*, 319.
(11) Lesiecki, M. L.; Shirk, J. S. *J. Chem. Phys.* **1972**, *56*, 4171.
(12) Schnöckel, V. Hg. *Z. Anorg. Allg. Chem.* **1976**, *424*, 203.
(13) Klemperer, W. *J. Chem. Phys.* **1956**, *24*, 353.
(14) Konings, R. J. M.; Booij, A. S. *J. Chem. Thermodyn.* **1992**, *24*, 1181.
(15) Adams, D. M.; Churchill, R. G. *J. Chem. Soc. A* **1970**, 697.
(16) Adams, D. M.; Churchill, R. G. *J. Chem. Soc. A* **1968**, 2141.
(17) Webb, D. U.; Justice, B. H.; Prophet, H. *J. Chem. Thermodyn.* **1969**, *1*, 227.
(18) Selivanov, G. K.; Mal'tsev, A. A. *J. Struct. Chem.* **1973**, *14*, 889.
(19) Perov, P. A.; Nedyak, S. V.; Mal'tsev, A. A. *Vestn. Mosk. Univ., Ser. 2 Khim.* **1974**, *15*, 201.
(20) Shirk, J. S.; Shirk, A. E. *J. Chem. Phys.* **1976**, *64*, 910.
(21) Palmer, K. J.; Elliott, N. *J. Am. Chem. Soc.* **1938**, *60*, 1852.
(22) Akishin, P. A.; Rambidi, N. G.; Zasorin, E. Z. *Kristallografiya* **1959**, *4*, 167.
(23) Zasorin, E. Z.; Rambidi, N. G. *J. Struct. Chem.* **1967**, *8*, 347.
(24) Shen, Q. Ph.D. Thesis, Oregon State University, Corvallis, OR, 1974.
(25) Spiridonov, V. P.; Gershikov, A. G.; Zasorin, E. Z.; Popenko, N. I.; Ivanov, A. A.; Ermolayeva, L. I. *High Temp. Sci.* **1981**, *14*, 285.
(26) Hargittai, M.; Kolonits, M.; Gödörházy, L. *Chem. Phys. Lett.* **1996**, *257*, 321.
(27) Ystenes, M.; Rytter, E.; Menzel, F.; Brockner, W. *Spectrochim. Acta A* **1994**, *50*, 233.
(28) Ystenes, M.; Westberg, N.; Ehrhardt, B. K. *Spectrochim. Acta A* **1995**, *51*, 1017.
(29) Berksoy, E. M.; Whitehead, M. A. *J. Chem. Soc., Faraday Trans. 2* **1988**, *84*, 1707.
(30) Curtiss, L. A. *Int. J. Quantum Chem.* **1978**, *14*, 709.
(31) Horn, H.; Ahlrichs, R. *J. Am. Chem. Soc.* **1990**, *112*, 2121.
(32) Hargittai, I.; Hargittai, M. *J. Chem. Phys.* **1974**, *60*, 2563.
(33) Beattie, I. R.; Blayden, H. E.; Ogden, J. S. *J. Chem. Phys.* **1976**, *64*, 909.
(34) Shen, Q.; Hedberg, K. *J. Phys. Chem. A* **1998**, *102*, 6470.
(35) Hagen, K.; Hedberg, K. *J. Am. Chem. Soc.* **1973**, *95*, 1003.
(36) Gundersen, G.; Hedberg, K. *J. Chem. Phys.* **1969,** *51*, 2500.
(37) Hedberg, L. *Abstracts of Papers, Fifth Austin Symposium on Gas-Phase Molecular Structure*, Austin, TX, March 1974, p 37.
(38) Ross, A. W.; Fink, M.; Hilderbrandt, R. *International Tables of Crystallography*; Kluwer Academic Publishers: Dordrecht 1992; Vol. 4, p 245.
(39) Frisch, M. J.; Trucks, G. W.; Schlegel, H. B.; Gill, P. M. W.; Johnson, B. G.; Robb, M. A.; Cheeseman, J. R.; Keith, T.; Petersson, G. A.; Montgomery, J. A.; Raghavachari, K.; Al-Laham, M. A.; Zakrzewski, V. G.; Ortiz, J. V.; Foresman, J. B.; Cioslowski, J.; Stefanov, B. B.; Nanayakkara, A.; Challacombe, M.; Peng, C. Y.; Ayala, P. Y.; Chen, W.; Wong, M. W.; Andres, J. L.; Replogle, E. S.; Gomperts, R.; Martin, R. L.; Fox, D. J.; Binkley, J. S.; Defrees, D. J.; Baker, J.; Stewart, J. P.; Head-Gordon, M.; Gonzalez, C.; Pople, J. A. *GAUSSIAN94*, Revision D.4: Gaussian, Inc., Pittsburgh, PA, 1995.
(40) Wadt, W. R.; Hay, P. J. *J. Chem. Phys.* **1985**, *82*, 284.
(41) Hedberg, L.; Mills, I. M. *J. Mol. Spectrosc.* **1993,** *160*, 117.
(42) Friesen, D.; Hedberg, K. *J. Am. Chem. Soc.* **1980**, *102*, 3987.
(43) Hedberg, K.; Iwasaki, M. *Acta Crystallogr.* **1964**, *17*, 529.
(44) Fischer, W.; Rhalfs, O. *Z. Anorg. Allg. Chem.* **1932**, *205*, 1.
(45) For example, see Fink, M.; Kohl, D. A. In *Stereochemical Applications of Gas-Phase Electron Diffraction. Part A- The Electron Diffraction Technique*; Hargittai, I., Hargittai, M., Eds.; VCH Publishers: NY, 1988; p 148.
(46) Pauling, L. *The Nature of the Chemical Bond*, 3rd ed.; Cornell University Press: Ithaca, NY, 1960; Chapter 7.
(47) Schomaker, V.; Stevenson, D. P. *J. Am. Chem. Soc.* **1941**, *63*, 37.